

Systematic fatigue spectrum editing by fast wavelet transform and genetic algorithm

Mohamad Mohseni¹ | Sridhar Santhanam¹  | Jesse Williams² |
Ash Thakker² | C. Nataraj^{1,3}

¹Department of Mechanical Engineering,
Villanova University, Villanova,
Pennsylvania, USA

²Global Technology Connection, Inc.,
Atlanta, Georgia, USA

³Villanova Center for Analytics of
Dynamic Systems, Villanova University,
Villanova, Pennsylvania, USA

Correspondence

Sridhar Santhanam, Department of
Mechanical Engineering, Villanova
University, Villanova, PA 19085, USA.
Email: sridhar.santhanam@villanova.edu

Funding information

NAVY STTR

Abstract

Fatigue testing is critical in order to establish the service life of load-bearing components and structures. The extensive time associated with full fatigue spectrum testing can lead to prohibitive costs. A significant need exists for a fatigue load spectrum editing methodology, based on the mechanics of fatigue, that produces load spectra that can replicate service damage in laboratory testing and can lead to compressed testing times and reduced costs. In this work, a wavelet genetic (WAVEGEN) algorithm is developed to edit fatigue loading spectra using wavelet analysis to greatly reduce the length of a spectrum while retaining the same damage accumulation characteristics. In addition, an optimization protocol using a genetic algorithm is included within this process to automatically select the best wavelet editing parameters. The algorithm is designed to identify the most suitable wavelet type, filter, and level to optimally edit a given fatigue spectrum and ensure equivalence between edited and unedited spectra from a damage perspective. The algorithm was applied to two well-known aircraft fatigue spectra: Fighter Aircraft Loading Standard for Fatigue evaluation (FALSTAFF) and Transport Wing Standard (TWIST). The proposed approach has demonstrated that both spectra can be compressed significantly even while ensuring equivalence from a damage perspective.

KEYWORDS

fatigue analysis, genetic algorithm, signal processing, wavelet transform

1 | INTRODUCTION

Aerospace components and structures are subject to fatigue loading throughout their service life. Such loads can cause progressive and permanent damage accumulation in the microstructure of materials. This damage accumulation can result in the formation of incipient cracks that eventually leads to critical crack growth and total failure of the structure. Fatigue testing therefore becomes important in order to establish the service life of critical load-bearing components and structures.¹

Most fatigue tests are conducted in the laboratory either on lab-scale or full-scale structures. Economic considerations dictate that a significant number of these tests are performed with a simplified, equivalent version of the actual service load spectrum. Equivalent fatigue loads are determined using established models (stress-life, strain-life, crack-growth rate, etc.²), empirical magnification factors, and many assumptions. While this approach has served its purpose, accurate service life determination of critical load bearing structures from laboratory testing requires a faithful reproduction of service load spectra

and even full-scale testing of the structure under consideration.

The load-time histories associated with many practical service fatigue loads possess characteristics that change as a function of time. If these are to be faithfully captured in the laboratory, the extensive time associated with fatigue testing can lead to prohibitive costs. Fatigue load spectrum editing is therefore imperative in order to reduce the time and costs. Accelerated testing in the laboratory has been practiced for many years. Traditional methods have included increasing the frequency of testing loads, increasing load amplitudes, and the removal of low amplitude load cycles that are perceived to be irrelevant.³ These methods are, in many cases, ad hoc in nature and quite often fail to replicate accurately the damage that is seen in real structures exposed to real service loads. A need exists for a fatigue load spectrum editing methodology, based on the mechanics of fatigue, that produces load spectra that can replicate service damage in laboratory testing and can also lead to compressed testing times and reduced testing costs.

In order to compress fatigue testing times, the fatigue load time history has to be analyzed to identify those portions that cause significant fatigue damage and eliminate sections that are insignificant in nature. Signal processing methods can play a crucial role in this effort. For instance, Fourier analysis can be used to decompose the signal into its frequency spectrum and identify frequencies with low amplitudes. However, this does little to enable signal time compression. Service fatigue load time histories are non-stationary in nature; signal characteristics change with time and this fact can be exploited. Wavelet transforms (WTs) and short-time Fourier transforms (STFTs) can be used to analyze nonstationary signals to identify those portions of the time history that cause significant fatigue damage. These pertinent portions can be extracted out of the overall time history and concatenated to produce a condensed or compressed history that can be used to accelerate laboratory fatigue testing.

Practically, for accelerating fatigue tests and reducing operating costs, various signal editing methods are developed and reported as time-domain method, S-transform, STFT, continuous wavelet transform (CWT), and discrete-wavelet transform (DWT). Time-domain method was first introduced by Conle and Topper.^{4,5} Here, the low amplitude cycles below a threshold level are removed to determine the damage caused by each level of strain cycles in a variable amplitude loading history. The damage reduction is then compared with original fatigue test results. The time-domain model is actually the most used approach for spectrum editing process as reported in previous studies.^{6–13}

However, the time-domain method is not precise in predicting the fatigue damage. This is due to the lack of

frequency information in the time domain as low-frequency segments are necessary to calculate the fatigue damage. Thus, to engage the frequency domain, the time-frequency approach was applied by Abdullah et al¹⁴ using the S-transform method and by Abdullah et al¹⁵ using the STFT. Aside from the advantage of considering the frequency domain, the drawback of time-frequency approach is the fixed window size in both time and frequency domains. Since sudden changes happen in high-frequency parts in fatigue signals, the smaller window size in the frequency domain is essential. This indicates that the WT analysis is suitable due to the capability of defining smaller window size at high-frequency parts.

Wavelet analysis offers a very promising avenue for achieving accelerated fatigue testing. Some preliminary efforts, particularly in automotive¹⁶ and wind turbine fatigue testing,¹⁷ have demonstrated the opportunities that exist with fatigue signal compression. However, optimization strategies have not been adopted in a meaningful manner to achieve maximum signal compression using wavelet analysis. Significant opportunities exist for extending these ideas to aerospace fatigue testing, particularly in multiaxial loading configurations.^{18,19} A systematic wavelet analysis-based approach is possible for aerospace fatigue spectrum editing that preserves fatigue damage, minimizes testing times and costs, accounts for load interaction effects, and minimizes clipping.

In Putra et al,^{20,21} the CWT is applied where the strain signals measured at automotive suspension components were extracted based on the Morlet wavelet to identify damaging segments. Also the DWT is used in Abdullah et al²² and Oh²³ to compress the fatigue signal while retaining the fatigue damage of the edited signal compared to the original one. An issue associated with both continuous and discrete wavelet approaches in these works was that the lengths of edited signals are not consistent and are dependent on the original behavior of the signals. This issue is resolved in our work by employing an appropriate optimization strategy alongside with a robust editing process based on the DWT which will be discussed in detail.

The objective of this study is to develop an analytical approach grounded in fatigue theory that compresses a fatigue test spectrum using wavelet analysis. The editing process is designed to retain equivalent damage accumulation and results in edited spectra that can provide significant cost and time savings associated with fatigue testing. The fast wavelet transform (FWT) algorithm, fatigue spectrum editing, and signal editing process optimization are described in Section 2. In Section 3, the results generated by the proposed wavelet genetic (WAVEGEN) algorithm are presented and discussed. Concluding remarks are presented in Section 4.

2 | METHODOLOGY

The primary goal of this work is to develop a signal processing technique to achieve significant reductions in the time span of edited variable-amplitude fatigue load spectra while ensuring that damage produced by the edited and unedited spectra is substantially equivalent.

At first, an appropriate fatigue spectrum with a broad range of load levels, frequencies, and overloads is required for analysis. There are many candidate spectra including Fighter Aircraft Loading Standard for Fatigue evaluation (FALSTAFF),²⁴ Transport Wing Standard (TWIST),²⁵ HELIX, and FELIX.²⁶ The FALSTAFF spectrum is perhaps the oldest existing standardized spectrum available for fighter aircraft wing loading. The complete FALSTAFF load history is based on two hundred flights. The recorded FALSTAFF data are available in the form of successive peaks and troughs expressed as a complete sequence of integers. The data are also available in the form of joint probability distribution matrices and exceedance curve representations. Rainflow cycle counting can also be applied for reconstructing the random load history by placing the individual cycles on the rising half or falling half of the major cycle. In fact, the rainflow cycle counting data is sufficient for calculating the accumulated damage. However, for wavelet analysis and spectrum editing, the original load sequence is required. In addition, the complete load history of TWIST spectrum based on 4,000 flights (402,665 cycles) is also available in the form of successive peaks and troughs. The data are normalized between the values: 0.6 and 2.6. Note that the signal characteristics of FALSTAFF and TWIST spectra differ.

Our aim is to remove those parts of the load spectrum that contribute little to the damage. Damage can be estimated using two methods (stress-life and crack growth rate) for both original and edited signals to study the effect of signal editing on the total damage. In the stress-life method, the S-N curve, a suitable damage accumulation rule, and a cycle-counting method are employed to model the fatigue damage. In the fatigue crack growth method, suitable crack growth models can be used to determine the effect of a load spectrum on a pre-existing noncritical crack and calculate the number of cycles of the spectrum that cause the crack to grow to a critical size. For signal editing of the FALSTAFF and TWIST load histories, we use the WT method outlined in the next section.

2.1 | Fast wavelet transform

As is well known, Fourier theory provides the ability to express a time-varying signal as a sum of sines and

cosines and thus enables us to identify the frequencies inherent in the signal. With transient signals, however, Fourier expansion lacks time information, and there is no way to tell when the frequencies are present and how the frequency components change with time.

The above problem can be overcome by a time-windowed STFT which has a fixed time-frequency window. However, STFT is inaccurate to analyze signals having relatively wide bandwidths that change rapidly with time. The WT (wavelet analysis) overcomes this issue by utilizing a fully scalable modulated window. The window is shifted along the signal at which point the spectrum is calculated. This process is repeated with a varying window for every new cycle. The process hence results in a collection of time-frequency representations of the signal, all with different resolutions; WT is hence a multi-resolution analysis.

The WT is categorized into continuous and discrete approaches.²⁷ The CWT^{13,28–31} generally evaluates the signal with the scaled and translated version of a basic mother wavelet. This method is a highly redundant transform that discretizes the scales very smoothly so that the finer sampling of scales results in a highly accurate analysis of the signal. The advantages of this approach are precision localization of the transient parts and better oscillatory behavior characterization of the signal, which leads to a detailed time-frequency signal analysis. On the other hand, the DWT provides a sparse and discrete representation of the signal. That is, the important features of the signal are captured by DWT coefficients which result in compressing the signal while preserving the high-quality approximation form of the signal. In this case, the scale parameter is controlled by the decomposition level, and the translation parameter is proportional to the scale. The major difference between the CWT and DWT is how the scale parameter is discretized. The strict discretization of the scale and translation parameters in discrete form ensures that DWT is an orthonormal transform where the discrete-large coefficients are captured and the discrete-small coefficients as noises are identified and detached separately. Note that the term FWT is used to describe DWT when a filter is applied before the wavelet decomposition.³²

It is for the reasons enunciated above that we choose DWT rather than CWT for fatigue spectrum editing in this work. It should be noted that the primary objective of the research is to identify the parts of the fatigue spectrum with negligible effect on damage calculation; in DWT, these correspond to the high-pass coefficients. Hence, retaining the essential parts of the signal that contribute the most to fatigue damage would be accomplished by retaining the low-pass coefficients. The one-dimensional wavelet coefficient (C) calculation based on

the scaling (s) and translating (μ) parameters as well as the wavelet function (ψ) is shown in Equation (1). The dyadic-scale parameter (s) is related to the specified decomposition level j as ($s = 2^j$) and to the resolution as ($1/s$). This means with increasing the number of levels, the scale increases, and the resolution of the final edited signal decreases. The smaller the resolution, the more the high-frequency parts, and consequently, greater lengths of the original signal are dropped.

$$C(s, \mu) = \int_R f(t) \frac{1}{\sqrt{s}} \left(\frac{t - \mu}{s} \right) dt, \{ \mu = k2^j, (j, k) \in Z^2 \} \quad (1)$$

Figure 1 depicts the one-dimensional wavelet decomposition structure of a typical signal. At the first level, two sets of coefficients as approximation and detail coefficients are generated. These vectors are obtained by convolving the signal with the low-pass filter for approximation and the high-pass filter for detail. In the next level, the approximation coefficient is decomposed with the same algorithm and lower resolution. These scaling wavelet filters return the low-pass and high-pass filters as quadrature mirror filters associated with orthogonal or biorthogonal wavelet families. The red line shows the path commenced from the original signal to the edited signal at each decomposition level. In practice, the analyzing mother wavelet needs to be chosen from the following wavelet families: Daubechies, Coiflets, Symlets, Discrete Meyer, Biorthogonal, and Reverse Biorthogonal.

Parenthetically, it should be noted that there is no universally accepted method for choosing the mother wavelet function. In general, mother wavelets are characterized by properties such as orthogonality, compact support, symmetry, and vanishing moment which are considered to make an “optimal” choice³³ and to seek to achieve a level of similarity between the mother wavelet and the signal of interest. Qualitative approaches using visual inspection are the most popular; for some

applications, quantitative approaches have been proposed such as minimum descriptor length³⁴ and Shannon entropy measures.³⁵ In the present work, the appropriate wavelet type is chosen through an optimization process as will be outlined later.

Discrete wavelet analysis essentially performs signal decomposition into a hierarchical set of approximation and detail coefficients. In this work, the wavelet decomposition denotes a multilevel one-dimensional wavelet analysis at a specified level where the signal is decomposed to low-frequency and high-frequency parts along with a downsampling process to avoid winding up with double data as the original signal. The term one-dimensional refers to the fact that a signal is investigated here rather than, for instance, an image, which would require a two-dimensional analysis.

Further decomposition levels lead to breaking down of the signal into lower resolution components as shown in Figure 2. For illustration, the original signal considered here is a small portion of the FALSTAFF spectrum with 1,000 cycles and is decomposed to three levels by DWT. At the first decomposition level, the WT identifies the low-frequency parts in 50% of the length of the original signal. This becomes then the signal input for subsequent decomposition at the next level. Further levels drop more high-frequency parts, and so on. In the second level, the edited signal is shortened to 25%, and in the third level, to around 12.5%. As can be seen, the edited signals keep the trend of the original signal well and capture significant peaks and troughs of the signal which are crucially important for the calculation of the total damage. It is important to note that the suitable number of levels depends on the nature of the signal and the maximum decomposition level is determined by the signal length and the type of mother wavelet applied.

Figure 3 shows the comparison between an original signal which is a typical 1,000 cycles of the FALSTAFF spectrum and the edited signal generated by a WT at the

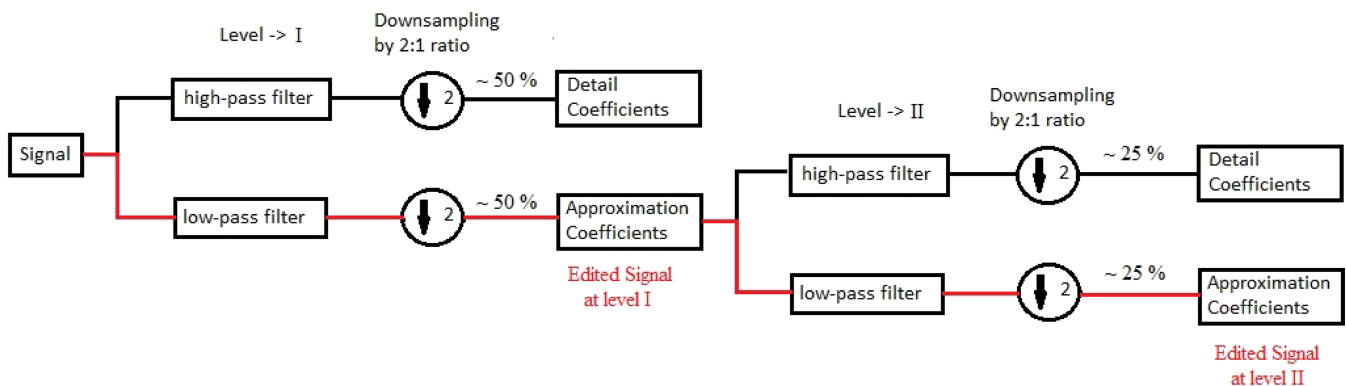


FIGURE 1 One-dimensional multilevel wavelet decomposition of a signal [Colour figure can be viewed at wileyonlinelibrary.com]

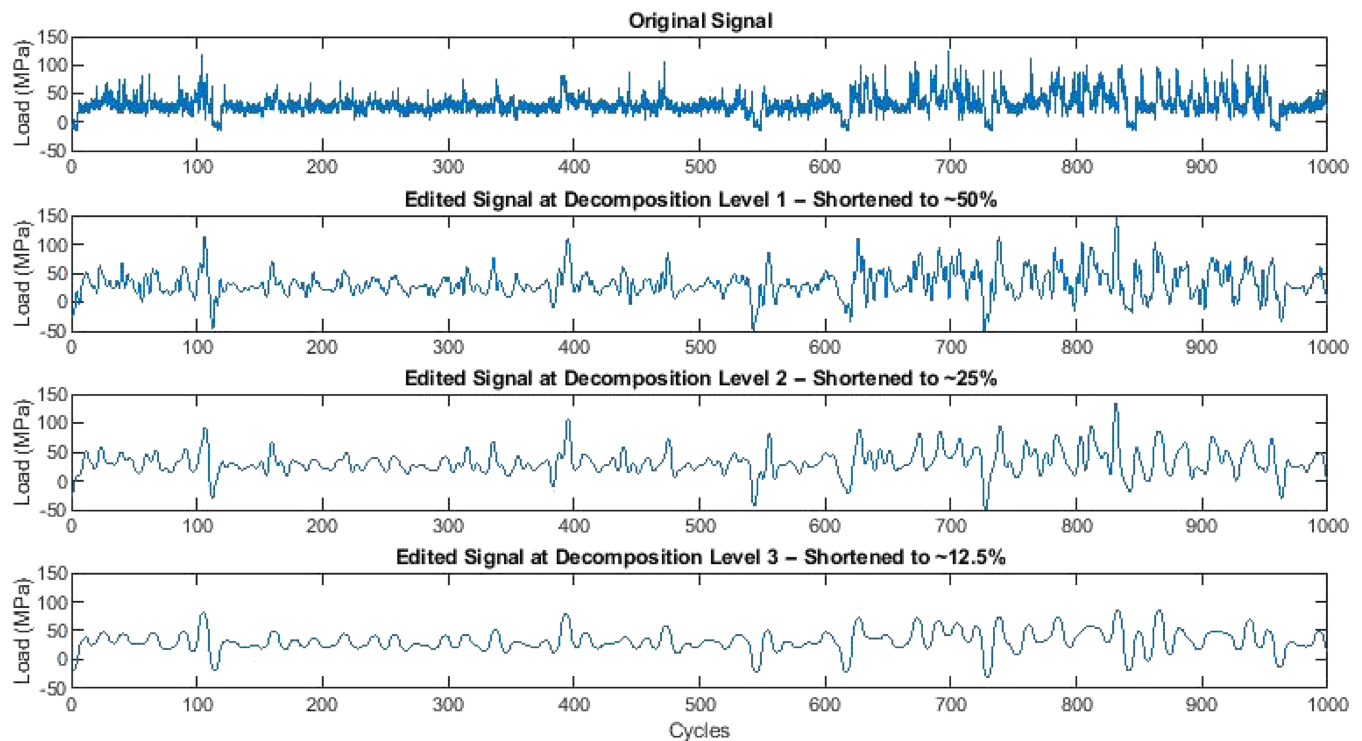


FIGURE 2 Original vs. edited signals at three decomposition levels for a portion (1,000 cycles) of the FALSTAFF spectrum [Colour figure can be viewed at wileyonlinelibrary.com]

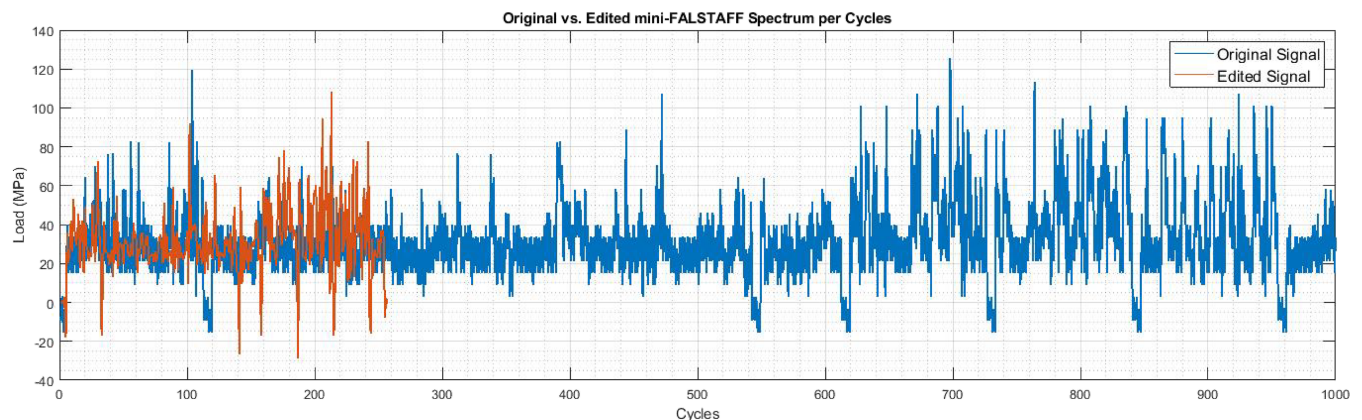


FIGURE 3 Comparing original signal vs. compressed edited signal for a portion (1,000 cycles) of the FALSTAFF spectrum; the edited signal is based on the Reverse Biorthogonal wavelet [Colour figure can be viewed at wileyonlinelibrary.com]

second level of decomposition. In this case, the Reverse Biorthogonal mother wavelet in the order of 1.3 is used. With this choice of the mother wavelet type and the decomposition level, and given the nature of the original signal, the low-frequency parts of the signal get identified and are shown as the red line in Figure 3. It is worth noting that the term “signal shortening” refers to the reduction of the number of cycles in the edited signal. As can be seen in Figure 3, the compressed signal in the second level of decomposition is 25% of the original signal.

2.2 | Fatigue spectrum editing

The basic fatigue behavior of metals and alloys as described by the S-N curve is commonly determined by constant amplitude, zero-mean, loading, and testing in the laboratory. However, most structures, especially aerospace structures, experience variable amplitude loading with nonzero mean stresses, when in service. Fatigue life of structures is strongly dependent on loading sequences and interactions, as well as stress amplitudes. Hence,

real-life variable amplitude fatigue load spectra are required for multiple purposes including: (a) to test small-scale or full-scale structures in the laboratory and (b) to numerically evaluate the fatigue life of test materials and structures using well-established analytical methods such as stress life and strain life. Many standardized fatigue load spectra have been developed and adopted for diverse applications. There are three well-established approaches to estimate the fatigue life of components and structures that are exposed to variable amplitude fatigue load spectra: stress-life, strain-life, and fatigue crack growth modeling. Both the stress-life and strain-life methods are used to predict life until the formation or nucleation of a crack. Stress life is frequently used for high-cycle fatigue situations, while strain life is preferred in low-cycle fatigue situations where plastic deformation is experienced in regions of stress concentration undergoing fatigue loading. Fatigue crack-growth life estimations are driven by a fail-safe design paradigm in which inspection periods are predetermined. In this approach, a nucleated crack is assumed to grow until it reaches a critical length that causes complete failure.

In stress-life modeling, first, the S-N curve obtained from constant stress amplitude, zero mean-stress, and cyclic fatigue load tests of a typical material are identified. Then, an appropriate model for non-zero mean stress calculation (such as Modified-Goodman, Gerber, Soderberg, etc.) is applied. In addition, a cycle counting method that relates a variable amplitude service load history to constant amplitude laboratory test results is used. The total damage is then determined by cumulative damage of the cycles. The S-N curves for most aerospace alloys in service are well established and available in the public domain. To account for nonzero mean stress effects in the fatigue test spectrum and the cycle counting method, the Modified-Goodman approach and the rainflow method are used here, respectively. In the stress-life approach, the damage is defined as the fraction of useful life of a component or structure that is consumed by the occurrence of a single event such as a single cycle of a cyclically varying applied load. Cumulative damage, D , is calculated by breaking up the applied variable amplitude fatigue load history into a sequence of events and combining the damage associated with each event. In principle, the cumulative damage D can be evaluated using linear and nonlinear models. The Palmgren-Miner rule is the most often used linear model which is used here. Although this method makes many assumptions that are violated, its simplicity is appealing and effective.

The stress-life methodology described above is applied to calculate the cumulative damage produced in a standard aerospace alloy that is exposed to the unedited test

spectrum as well as the edited test spectrum. If the “unedited” and the “edited” cumulative damage metrics are within 5% of each other, the two test spectra will be considered to be equivalent. This is captured by the damage error percentage metric in Equation (2); if the value of this metric is less than 5%, then the edited and unedited fatigue spectra are considered equivalent from a damage perspective. The stress-life approach neglects sequence effects in loading and their impact on damage.

$$DEP = \left| \frac{D_O - D_E}{D_O} \right| \times 100 \quad (2)$$

where D_O is the damage caused by the entire original spectrum and D_E is the damage caused by the edited spectrum. DEP is the damage error percent metric.

The application of wavelet based editing of fatigue spectra to generate equivalent edited spectra is explored next. The FALSTAFF spectrum is first considered for study. For our analysis, we chose the material, Al 6061-T6. This alloy has an ultimate strength of 320 MPa and a fatigue strength of 80 MPa for 1.0×10^7 cycles of reversed stress. Fatigue test spectra such as FALSTAFF and TWIST are typically available as a sequence of normalized, scaled numbers. To convert such spectra into a typical stress spectrum, a suitable stress scaling factor has to be chosen. For the purposes of our analysis, we chose a stress scaling factor that ensured a maximum stress of 90 MPa for the FALSTAFF spectrum, in order to ensure reasonable damage and life calculations for the chosen material of Al 6061-T6.

Instead of using the entire FALSTAFF spectrum, a portion of the spectrum is extracted and then subjected to our editing methodology for illustrative purposes. The extract from the FALSTAFF spectrum considered for study is 1,000 cycles (10,000–11,000) long. Tables 1 and 2 illustrate the damage error percentage values for the spectrum extract using various filter and wavelet types at two levels which result in the spectrum extract being edited to 50% and 25% of the original length, respectively. In these tables, the first column displays the various filter types; the first row depicts the varied wavelet types. The cell entries in bold indicate the desired damage error percentage values beneath 5%.

Figure 4 displays the comparison of the original, edited and compressed-edited signals for an extracted case from Table 2 which is for 1,000 cycles (10,000–11,000) of the FALSTAFF spectrum, with filter type as “bior3.9” and Wavelet type as “rbio1.3” at the second decomposition level. This combination results in a signal shortening of 75% with the damage error percentage being 1.3%. In the figure, the blue line is the original spectrum, the red line is the edited spectrum, and the

TABLE 1 Damage error percentage values for the original and edited spectrum for a 1,000-cycle (10,000–11,000) long extract from the FALSTAFF spectrum; wavelet editing was performed at level 1 decomposition

Filter	Wavelet	rbio1.3	rbio1.5	sym2	sym4	sym8	coif2	coif4	coif5	db2	db3	db4	db5	db6	db7
bior3.1		31.9	16.9	123.8	80.2	8.3	95.8	22.5	7.6	123.8	53.5	56.7	42.8	46.8	61.9
bior3.3		61.9	56.5	27.8	11.9	35.6	18.9	27.5	37.3	27.8	11.8	76.2	76.1	75.8	82.2
bior3.5		67.7	63.8	4.5	5.7	46.3	1.2	39.4	47.5	4.5	28.2	79.8	80.9	79.4	85.2
bior3.7		70.9	67.6	8.7	16.1	52.5	12.9	46.3	53.3	8.7	37.5	81.9	83.5	81.5	86.5
bior3.9		73.0	70.2	16.3	23.2	56.8	20.9	51.0	57.3	16.3	42.9	83.0	85.3	83.1	87.4

TABLE 2 Damage error percentage values for the original and edited spectrum for a 1,000-cycle (10,000–11,000) long extract from the FALSTAFF spectrum; wavelet editing was performed at level 2 decomposition

Filter	Wavelet	rbio1.3	rbio1.5	sym2	sym4	sym8	coif2	coif4	coif5	db2	db3	db4	db5	db6	db7
bior3.1		3.4	87.5	536.2	133.4	2.2	301.6	58.2	39.0	536.2	455.6	147.4	19.0	63.8	61.1
bior3.3		74.4	50.0	16.5	31.8	74.6	26.1	68.0	71.5	16.5	34.0	73.9	82.8	79.6	76.8
bior3.5		27.8	41.3	360.2	89.0	17.6	216.6	15.6	1.6	360.2	271.6	39.7	45.8	34.8	23.4
bior3.7		88.7	80.7	24.7	75.9	88.1	66.5	85.8	87.4	24.7	55.9	83.5	90.7	88.9	89.0
bior3.9		1.3	100.6	605.1	166.8	18.4	333.8	54.3	27.7	605	416	92.2	27.3	14.7	0.4

black line is the compressed-edited spectrum. The latter compares the edited spectrum to the original one demonstrating how much truncation occurs after the signal reduction. DEP denotes the damage error percentage value, the decomposition level is designated as L, the filter type as F, and the wavelet type as W.

The main outcome of the effort reflected in Tables 1 and 2 is to obtain the desired solutions that are based on different filter types, wavelet types, and decomposition levels. A huge amount of effort is required to check all possible solutions to find out which combinations lead to acceptable results. An acceptable result is defined as one where the edited signal is shorter than the unedited signal, but the damage caused by both is equivalent. Equivalency of damage is established by ensuring that the damage percent difference between the edited and unedited spectra is less than 5%. Instituting an automated optimization procedure to identify the most suitable compressed signal is imperative in order to reduce the effort involved. This was the motivating reason to improve the spectrum editing process by implementing an appropriate optimization method which will be discussed next.

2.3 | Signal editing process optimization with GA

As demonstrated earlier, the various design parameter combinations present nondeterministic and disordered solutions depending on the nature of the original signal without a clearly identifiable trend. This inability to easily identify algorithmic parameters suggests that we seek an automated algorithm that implements optimization. This strategy would enable the editing process to lead to the desired solution in a significantly shorter time than manually checking all potential solutions. Among a

variety of optimization techniques, the genetic algorithm (GA)³⁶ is a proper choice to consider based on the unique problem characteristics. Note, in addition, that the editing process includes discrete variables (such as filter types, wavelet types and decomposition levels), and our past experience^{37–41} has shown that GA is a robust optimization tool to resolve exactly these kinds of integer optimization problems.

A very brief overview of the GA is provided here. The GA is first constructed by its biological criterion, then mathematically formulated and implemented in MATLAB. At first, the GA creates a random initial population, and then it generates a sequence of new populations. At each step, the algorithm uses individuals in the current generation to create the next population. In order to create the new population, the GA first scores each member of the current population by computing its fitness value that is called raw fitness score. Then, the GA scales the raw fitness scores to convert them into a more usable range of values which are called expectation values. Next, it selects members called parents based on their expectation. Some of the individuals in the current population that have lower fitness are chosen as elites, which are passed to the next population. Afterward, it produces children from the parents by making random changes to a single parent (mutation) or by combining the vector entries of a pair of parents (crossover). Then, it replaces the current population with the children to form the next generation.⁴²

The fitness function or the objective function of the optimization problem is the target function to be minimized. An individual is a vector of design variables that is applied to the fitness function, and the value of fitness function for an individual is its score. A population is an array of individuals where the same individual can appear more than once in the population. At each

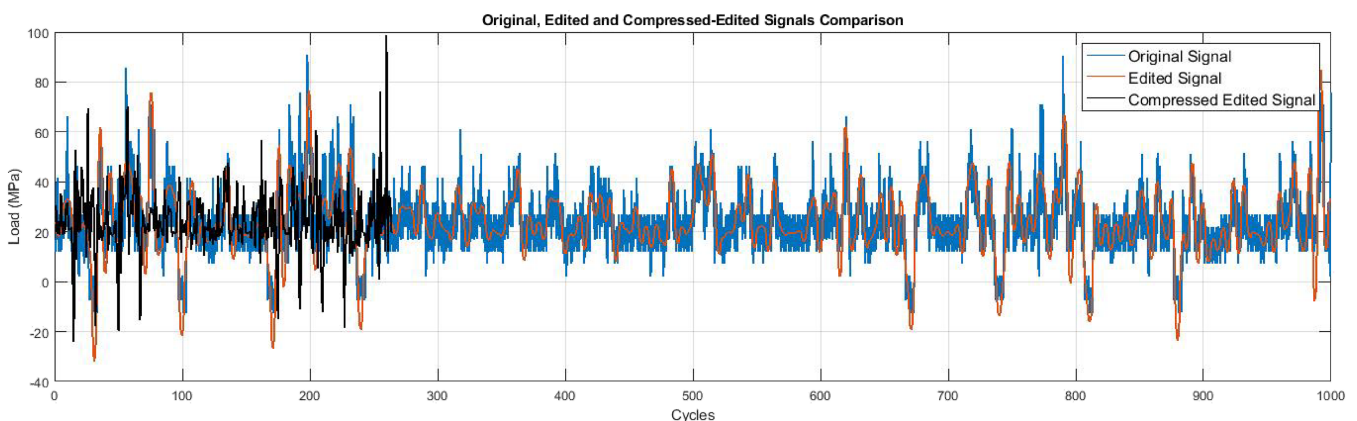


FIGURE 4 Signal comparison for 1,000 cycles (10,000–11,000) with DEP: 1.3, L: 2, F: bior3.9, W: rbio1.3 [Colour figure can be viewed at wileyonlinelibrary.com]

iteration, the GA performs a series of computations on the current population to produce a new population. Each successive population is called a new generation. The fitness value of an individual is the value of the fitness function for that individual. Because the algorithm finds the minimum of the fitness function, the best fitness value for a population is the smallest fitness value for any individual in the population. The algorithm ends when one or more of the stopping criteria such as the number of generations, fitness limit, function tolerance, and constraint tolerance are met.⁴²

For our implementation of GA on the fatigue spectrum editing process,

- the objective function is the length of the edited signal (which needs to be minimized), or equivalently, the decomposition level, which needs to be maximized;
- the constraint that we specify here is that the difference (or error) between the damage due to the original and that due to edited signals should be less than 5%;
- the design variables for our process are filter types, wavelet types, and decomposition levels.

3 | RESULTS AND DISCUSSION

The automation and optimization of the wavelet-based signal editing process with the application of a GA are applied to the FALSTAFF and TWIST loading spectra to demonstrate the algorithm's capabilities. This wavelet-based signal editing process coupled with a GA optimization scheme is labeled WAVEGEN.

The FALSTAFF and TWIST loading spectra contain approximately 18,000 and 400,000 cycles, respectively. The WAVEGEN algorithm automatically optimizes various types of filters and wavelets as well as different

decomposition levels. The maximum decomposition level is set to 4, which means the signal reduction is limited to a maximum of 93.75%.

The WAVEGEN algorithm is first applied to the complete FALSTAFF spectrum. Figure 5 shows the comparison between original and edited FALSTAFF spectrum (original has 18,000 cycles) with damage error difference of 2.25% and signal reduction of 87.5%. These optimized values are generated by WAVEGEN with filter type as “bior4.4” and Wavelet type as “rbio3.3” at the third decomposition level.

Figure 6 shows the comparison between original and edited TWIST spectrum (original has 400,000 cycles) with damage error difference of 4.23% and signal reduction of 75%. The edited spectrum is the optimized edited spectrum generated by WAVEGEN with filter type as “bior3.9” and wavelet type as “rbio3.7” at the second decomposition level.

For the spectra considered in Figures 5 and 6, since the real test spectra have generally a large length and stochastic transient terms, the editing performed by WAVEGEN has limitations that can be improved upon by performing the editing in blocks. So this limitation of single spectrum editing is the motivation to develop the Block-WAVEGEN algorithm which will be discussed next.

3.1 | Block-GA wavelet editing

The proposed WAVEGEN algorithm is extended to discretize the original spectrum into several blocks according to the signal length and apply the editing process coupled with the GA for each block. In this case, the best wavelet optimization design parameters that match with each specific block are selected rather than the same

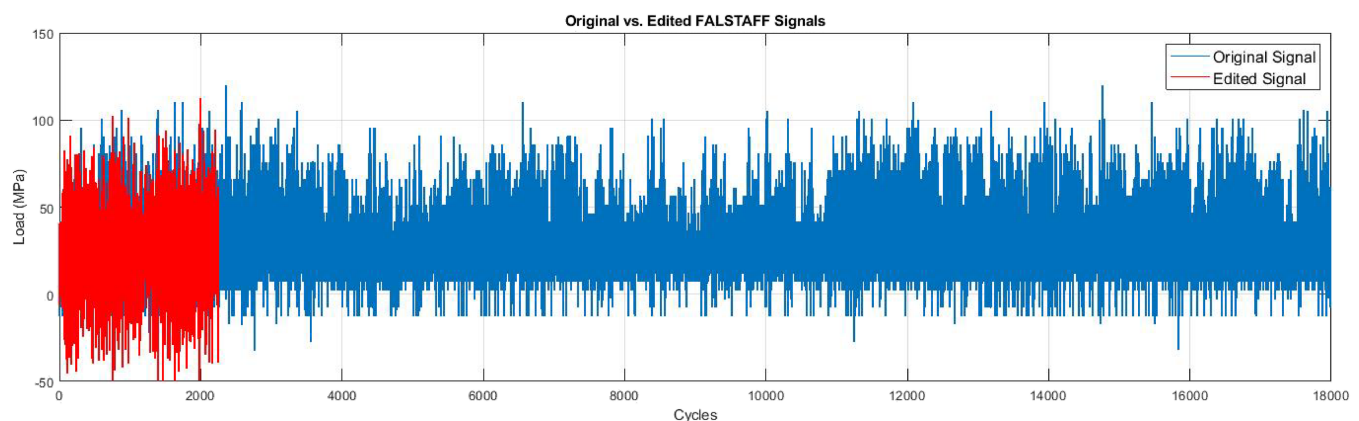


FIGURE 5 Comparison of original and edited FALSTAFF spectrum with 87.5% signal reduction [Colour figure can be viewed at wileyonlinelibrary.com]

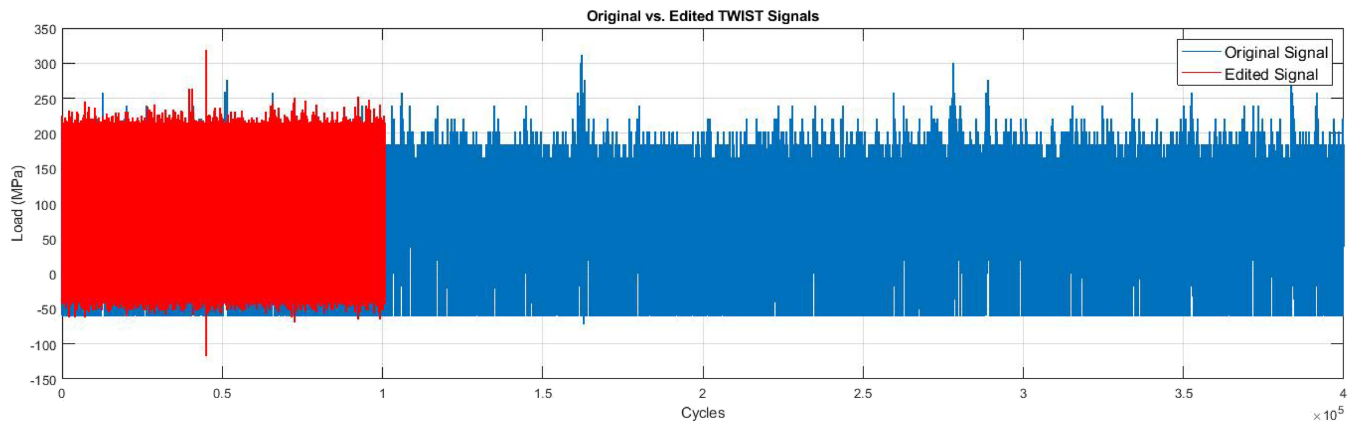


FIGURE 6 Comparison of original and edited TWIST spectrum with 75% signal reduction [Colour figure can be viewed at wileyonlinelibrary.com]

TABLE 3 Block-WAVEGEN results for FALSTAFF spectrum for block size of 6,000 cycles

Block No.	Cycles	Filter	Wavelet	Decomposition	Signal red (%)	Damage diff (%)
1	6,000	bior3.3	rbio6.8	3	87.5	1.35
2	6,000	bior3.9	rbio6.8	4	93.75	4.56
3	5,983	bior3.9	db2	3	87.5	4.19
—	17,983	—	—	Averaged —>	89.6	3.37

ones for the whole spectrum. This innovation makes the spectrum editing process very effective and practical.

Further, since each block with its own specific intrinsic behavior could attain a specific length reduction based on the decomposition level, with the maximum decomposition level being 4, the overall reduction would be within the range 50%–93.75%. The application of our new Block-WAVEGEN approach is shown next as the results of editing the FALSTAFF and TWIST spectra.

3.2 | Analysis of FALSTAFF spectrum

A detailed analysis is presented next of the editing of the FALSTAFF spectrum using wavelet transformation and GA optimization for various block sizes. A wide range of block sizes are considered ranging from the full size of 18,000 to a block size of 1,500 cycles. Tables 3–5 illustrate the optimized editing process results generated by GA for various block size selections to investigate the effect of block size on the final signal reduction and damage difference percentages between the original and edited FALSTAFF spectrum.

Table 3 shows the results obtained by the use of three blocks of about 6,000 cycles each, leading to a signal reduction of 90% while the damage difference is still under 5%. As can be seen, the optimization process

returns different filter and wavelet types as well as decomposition levels for the blocks.

The best signal reduction results are achieved with block size extracts of 4,500 and 3,000 cycles. Table 4 provides the results for a block size of 3,000 cycles. In this case all blocks attain the assumed maximum signal reduction value of 93.75% while the damage difference percentages of all blocks are under 5% as specified. It is not intuitively clear why this situation occurs for this specific block size, but it is clear that the signal characteristic plays an important role to determine the appropriate filter and wavelet types for any given block.

In Table 5, a block size of 1,500 cycles is considered leading to 12 blocks in the whole FALSTAFF spectrum. The GA was able to find the maximum signal reduction for each block where the damage difference is less than 5% and the averaged signal reduction and damage difference percentages for the entire spectrum are 88% and 2.3%, respectively. This indicates that the signal reduction range is between 75% and 93.75%. It could also be remarked that the variety of wavelet types (as Daubechies, Coiflets, Symlets, and Reverse Biorthogonal) that emerge as the optimal signal editing tools are because of the variations in the FALSTAFF spectrum.

Figure 7 compares the signal reduction and damage difference percentages for a range of block sizes which are carried out on the FALSTAFF spectrum and generated by

TABLE 4 Block-WAVEGEN results for FALSTAFF spectrum for block size of 3,000 cycles

Block No.	Cycles	Filter	Wavelet	Decomposition	Signal red (%)	Damage diff (%)
1	3,000	bior3.7	rbio3.5	4	93.75	2.97
2	3,000	bior3.9	rbio2.6	4	93.75	4.98
3	3,000	bior3.1	dmey	4	93.75	0.81
4	3,000	bior3.1	db10	4	93.75	3.64
5	3,000	bior3.1	sym7	4	93.75	4.46
6	2,983	bior1.5	rbio2.2	4	93.75	3.89
—	17,983	—	—	Averaged —>	93.75	3.46

TABLE 5 Block-WAVEGEN results for FALSTAFF spectrum for block size of 1,500 cycles

Block No.	Cycles	Filter	Wavelet	Decomposition	Signal red (%)	Damage diff (%)
1	1,500	bior3.3	sym7	3	87.5	3.35
2	1,500	bior3.1	sym6	4	93.75	4.58
3	1,500	bior3.9	rbio2.6	4	93.75	4.28
4	1,500	bior3.9	rbio2.6	4	93.75	1.05
5	1,500	bior1.5	rbio3.3	4	93.75	0.57
6	1,500	bior2.2	db2	2	75.0	1.34
7	1,500	bior3.7	coif1	3	87.5	1.26
8	1,500	bior3.1	coif3	4	93.75	4.23
9	1,500	bior3.5	rbio2.6	4	93.75	0.68
10	1,500	bior3.3	rbio3.9	4	93.75	1.56
11	1,500	bior4.4	rbio2.6	2	75.0	2.24
12	1,483	bior4.4	rbio2.6	2	75.0	2.07
—	17,983	—	—	Averaged —>	88.0	2.27

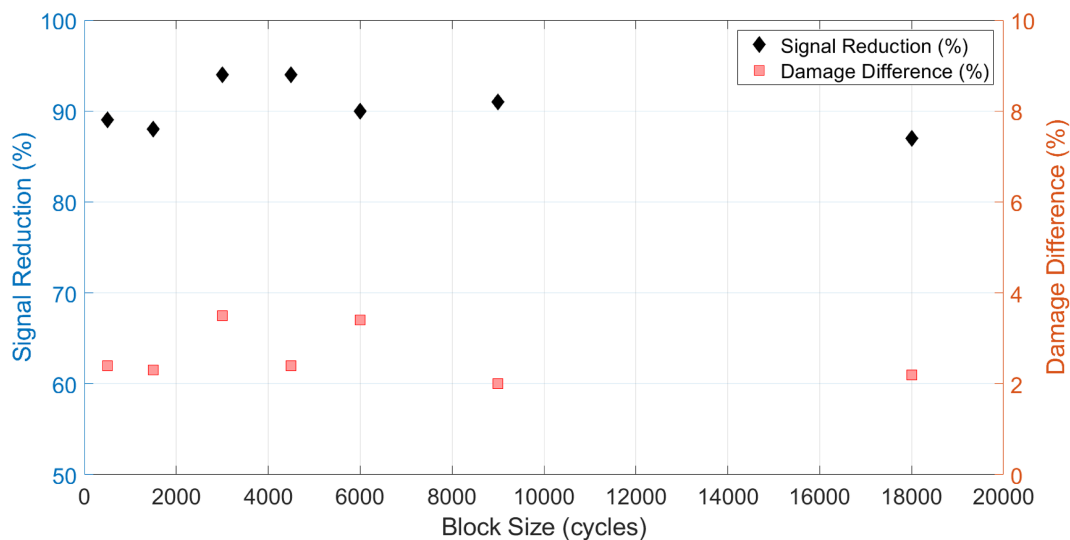


FIGURE 7 Signal reduction and damage difference percentages for various block sizes of FALSTAFF spectrum [Colour figure can be viewed at wileyonlinelibrary.com]

our block-based Wavelet-Genetic Algorithm Editing (B-WAVEGEN) approach. As can be seen, the damage difference percentage for each block size selection is under 5% as expected, but it cannot be implied that lower block size leads to an increase in the signal reduction.

3.3 | Analysis of TWIST spectrum

To check the capability and feasibility of the proposed B-WAVEGEN algorithm to handle other substantial fatigue spectrum signals, the B-WAVEGEN approach is also carried out for the TWIST spectrum as demonstrated in Tables 6–8. The considered block sizes are 200,000, 100,000, and 50,000 cycles.

Table 6 shows the results of the editing process obtained by splitting the TWIST spectrum into two equal blocks of 200,000 cycles each. The signal reduction and damage difference percentages are at 81.25% and 1.92%, respectively.

Further assessment is done by splitting the TWIST spectrum into four blocks of 100,000 cycles as shown in Table 7. Varied types of filters and wavelets are achieved by the B-WAVEGEN algorithm for each block with average signal reduction of 62.5% and damage error percentage of 1.57%.

Table 8 illustrates the results of splitting the TWIST spectrum into eight blocks of 50,000 cycles. It can be seen that decreasing the block size leads to improvements in the signal reduction in some blocks. The average signal reduction and damage difference percentages calculated by the B-WAVEGEN algorithm are 75.8% and 3.36%, respectively.

In general, the wavelet type of Reverse Biorthogonal is listed for all block sections meaning this wavelet is the optimal choice for editing the TWIST spectrum. Again, this indicates that the wavelet type is strongly dependent on the nature of the spectrum. Regarding the signal reduction relation to the block size, the range of final signal reduction is between 50% and 93.75% so that a clear

TABLE 6 B-WAVEGEN results for TWIST spectrum for block size of 200,000 cycles

Block No.	Cycles	Filter	Wavelet	Decomposition	Signal red (%)	Damage diff (%)
1	200,000	bior3.7	rbio2.2	2	75.0	3.60
2	200,000	bior6.8	rbio3.1	3	87.5	0.24
—	400,000	—	—	Averaged —>	81.25	1.92

TABLE 7 B-WAVEGEN results for TWIST spectrum for block size of 100,000 cycles

Block No.	Cycles	Filter	Wavelet	Decomposition	Signal red (%)	Damage diff (%)
1	100,000	bior3.7	rbio3.9	1	50.0	1.93
2	100,000	bior3.3	rbio2.2	2	75.0	0.34
3	100,000	bior2.2	rbio3.1	1	50.0	3.78
4	100,000	bior3.7	rbio3.7	2	75.0	0.23
—	400,000	—	—	Averaged —>	62.5	1.57

TABLE 8 B-WAVEGEN results for TWIST spectrum for block size of 50,000 cycles

Block No.	Cycles	Filter	Wavelet	Decomposition	Signal red (%)	Damage diff (%)
1	50,000	bior3.5	rbio3.9	1	50.0	7.75
2	50,000	bior3.3	rbio3.7	2	75.0	1.39
3	50,000	bior3.1	rbio1.3	3	87.5	2.57
4	50,000	bior3.3	rbio2.2	2	75.0	4.85
5	50,000	bior6.8	rbio3.1	2	75.0	2.33
6	50,000	bior1.3	rbio3.1	4	93.75	3.93
7	50,000	bior1.5	rbio3.1	2	75.0	0.70
8	50,000	bior3.3	rbio3.9	2	75.0	3.34
—	400,000	—	—	Averaged —>	75.8	3.36

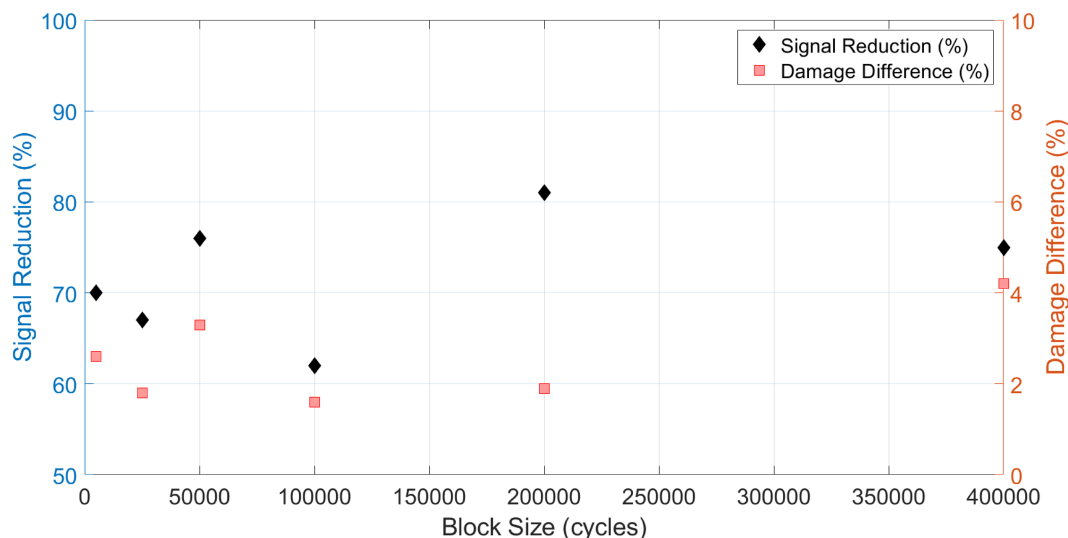


FIGURE 8 Signal reduction and damage difference percentages for various block sizes of TWIST spectrum [Colour figure can be viewed at wileyonlinelibrary.com]

relationship between the block size and signal reduction cannot be established mathematically.

Figure 8 compares the signal reduction and damage difference percentages for a range of block sizes which are carried out on the TWIST spectrum. As can be seen, the damage difference percentage for each block size selection of TWIST spectrum is under 5% as well. In a general comparison between Figures 7 and 8, the signal reduction related to FALSTAFF is higher than TWIST.

4 | CONCLUSIONS AND FUTURE WORK

In this work, a fatigue test spectrum editing algorithm is developed using WT and GA optimization (WAVEGEN) that can reduce cost and fatigue testing time schedule. The optimization process automatically selects the best wavelet fitting parameters which reduce the editing process time. To estimate the fatigue life of components under fatigue load spectrum, the stress-life model is employed. In stress-life model, the fatigue life calculation is performed using S-N curves, rainflow cycle counting technique, and the Palmgren–Miner rule. The generated edited spectrum by WAVEGEN achieves equivalent damage and retains key attributes as well as the main aspects of the original spectrum. The developed fatigue spectrum editing algorithm is successfully applied on FALSTAFF and TWIST spectra with significant signal reductions while maintaining a damage difference of less than 3% between unedited and edited spectrum. In order to refine the methodology, the ability to split the spectrum into blocks is added to the WAVEGEN editing process. Future

work will validate our analytical results with experimental fatigue tests performed under uniaxial loading. Aerospace alloys will be tested in a mechanical testing system using the original and edited loading spectrum, and the resultant fatigue lives will be compared. In addition, the algorithm's capabilities will be expanded to address multiaxial loading, proportional and non-proportional.

ACKNOWLEDGMENTS

This work was supported by an STTR grant from the Navy (N6833518C0747). The authors would like to acknowledge the assistance provided by Dieter Bender with the discrete wavelet transform.

AUTHOR CONTRIBUTIONS

Mohammad Mohseni implemented the WAVEGEN algorithm and authored the first draft of the manuscript. All other authors were involved with the development of the algorithm and the editing and revising of the manuscript to varying degrees. Sridhar Santhanam supervised the fatigue damage evaluations with input from Jesse Williams and Ash Thakker. C. Nataraj supervised the development of the WAVEGEN algorithm.

DATA AVAILABILITY STATEMENT

The data that support the findings of this study are available from the corresponding author upon reasonable request.

ORCID

Sridhar Santhanam  <https://orcid.org/0000-0002-0450-5191>

REFERENCES

1. Anderson TL. *Fracture Mechanics: Fundamentals and Applications*: CRC Press; 1995.
2. Ellyin F. *Fatigue Damage, Crack Growth and Life Prediction*. London: Chapman & Hall; 1997.
3. Farrar CR, Duffey TA, Cornwell PJ, Bement MT. A Review of Methods for Developing Accelerated Testing Criteria. In: Proceedings of SPIE; 2003.
4. Conle A, Topper TH. Evaluation of small cycle omission criteria for shortening of fatigue service histories. *Int J Fatigue*. 1979;1:23-28.
5. Conle A, Topper TH. Overstrain effects during variable amplitude service history testing. *Int J Fatigue*. 1980;2:130-136.
6. Phillips E. Effects of Truncation of a Predominantly Compression Load Spectrum on the Life of a Notched Graphite/Epoxy Laminate. In: Lauraitis K, ed. *Fatigue of Fibrous Composite Materials*: ASTM International; 1981:197-212.
7. Buch A. Effect of some aircraft loading program modifications on the fatigue life of open hole specimens. *Eng Fract Mech*. 1980;13:237-256.
8. Heuler P, Seeger T. A criterion for omission of variable amplitude loading histories. *Int J Fatigue*. 1986;8:225-230.
9. Lanciotti A, Lazzeri L. Effects of spectrum variations on fatigue crack growth. *Int J Fatigue*. 1992;14:319-324.
10. Stephens RI, Dindinger PM, Gunger JE. Fatigue damage editing for accelerated durability testing using strain range and SWT parameter criteria. *Int J Fatigue*. 1997;19:599-606.
11. Nyman T, Ansell H, Blom A. Effects of truncation and elimination on composite fatigue life. *Compos Struct*. 2000;48:275-286.
12. Ko SG, Oh CS, Choi BI. The elucidation of load history editing effect on fatigue crack growth by crack closure concept. *Int J Fatigue*. 2005;27:255-262.
13. Xiong JJ, Shenoi RA. A load history generation approach for full-scale accelerated fatigue tests. *Eng Fract Mech*. 2008;75:3226-3243.
14. Abdullah S, Nizwan CKE, Yunoh MFM, Nuawi MZ, Nopiah ZM. Fatigue features extraction of road load time data using the S-Transform. *Int J Autom Technol*. 2013;14:805-815.
15. Abdullah S, Nizwan CKE, Nuawi MZ. A study of fatigue data editing using short-time Fourier transform (STFT). *Am J Appl Sci*. 2009;6:565-575.
16. Husaini, Putrab TE, Ali N. The Morlet wavelet transform for reducing fatigue testing time of an automotive suspension signal. In: AIP Conference Proceedings; 1983.
17. Pratumnopharat P, Leung P, Court R. Wavelet transform-based stress-time history editing of horizontal axis wind turbine blades. *Renew Energy*. 2014;63:558-575.
18. Fatemi A, Shamsaei N. Multiaxial Fatigue: An overview and some approximation models for life estimation. *Int J Fatigue*. 2011;33:948-958.
19. You BR, Lee SB. A Critical Review on Multiaxial Fatigue Assessment on Metals. *Int J Fatigue*. 1996;18:235-244.
20. Putra TE, Abdullah S, Schramm D, Nuawi MZ, Bruckmann T. Reducing cyclic testing time for components of automotive suspension system utilising the wavelet transform and the Fuzzy C-Means. *Mech Syst Sig Process J*. 2017;90:1-14.
21. Putra TE, Abdullah S, Nuawi MZ, Nopiah ZM. Wavelet Coefficient Extraction Algorithm for Extracting Fatigue Features in Variable Amplitude Fatigue Loading. *J Appl Sci*. 2010;10:277-283.
22. Abdullah S, Choi JC, Giacomini JA, Yates JR. Bump extraction algorithm for variable amplitude fatigue loading. *Int J Fatigue*. 2006;28:675-691.
23. Oh CS. Application of wavelet transform in fatigue history editing. *Int J Fatigue*. 2001;23:241-250.
24. Mitchenko EI, Prakash RV, Sunder R. Fatigue Crack Growth under an Equivalent FALSTAFF spectrum. *Fatigue Fract Eng Mater Struct*. 1995;18:585-595.
25. de Jonge JB, Nederveen A. Effect of Gust Load Alleviation on Fatigue and Crack Growth in ALCLAD 2024-T3. *ASTM STP*. 1980;714:170-184.
26. Heuler P, Klatschke H. Generation and use of standardized load spectra and load-time histories. *Int J Fatigue*. 2005;27:974-990.
27. Addison PS. *The Illustrated Wavelet Transform Handbook: Introductory Theory and Applications in Science, Engineering, Medicine and Finance*: CRC Press; 2002.
28. Bender D, Jalali A, Nataraj C. Pilot study to predict cardiac arrest using continuous wavelet transform measures as predictors for an artificial neural network. In: IEEE Engineering in Medicine and Biology Society Conference; 2016.
29. Chui CK. Wavelets: A Mathematical Tool for Signal Analysis for Industrial and Applied Mathematics; 1997.
30. Gao RX, Yan R. *Wavelets - Theory and Applications for Manufacturing*: Springer; 2011.
31. Abdullah S. The Wavelet Transform for Fatigue History Editing: Is it Applicable for Automotive Applications? *J Eng Appl Sci*. 2007;2:342-349.
32. Mathworks. Wavelet Analysis Toolbox: User's Guide. r2018b.
33. Ngui WK, Leong MS, Hee LM, Abdelrhman AM. Wavelet Analysis: Mother Wavelet Selection Methods. *Appl Mech Mater*. 2013;393:953-958.
34. Saito N. Simultaneous noise suppression and signal compression using a library of orthonormal bases and the minimum description length criterion. In: Fofoula-Georgiou E, Kumar P, eds. *Wavelets in Geophysics*: Academic Press; 1994.
35. Yan R. Base wavelet selection criteria for non-stationary vibration analysis in bearing health diagnosis. University of Massachusetts Amherst; 2007.
36. Goldberg DE. *Genetic Algorithms in Search, Optimization, and Machine Learning*: Addison-Wesley Publishing Company; 1989.
37. Ferrese F, Dong O, Nataraj C, Biswas S. Optimal Feedback Control of Power Systems Using Eigenstructure Assignment and Particle Swarm Optimization. *Naval Eng J*. 2011;123:67-75.
38. Samanta B, Nataraj C. Use of Particle swarm optimization for machinery fault detection. *Eng Appl Artif Intell*. 2009;22:308-316.
39. Samanta B, Nataraj C. Application of particle swarm optimization and proximal support vector machines for fault detection. *Swarm Intell*. 2009;3:303-325.

40. Samanta B, Nataraj C. Design of Intelligent Ship Autopilots using Particle Swarm Optimization. In: 2008 IEEE Swarm Intelligence Symposium (SIS2008) IEEE; 2008.
41. Naseradinmousavi P, Nataraj C. Optimal design of solenoid actuators driving butterfly valves. *ASME J Mech Design*. 2013; 094501-5:135.
42. Mathworks. Global Optimization Toolbox: User's Guide. r2018b.

How to cite this article: Mohseni M, Santhanam S, Williams J, Thakker A, Nataraj C. Systematic fatigue spectrum editing by fast wavelet transform and genetic algorithm. *Fatigue Fract Eng Mater Struct*. 2022;45(1):69-83. doi: 10.1111/ffe.13583